MPInterconsulting

ULTRASONICS - SONOCHEMISTRY - INNOVATION

A SERIES OF EXTRAORDINARY AND UNIQUE BOOKS RECOMMENDED BY MPI

Some researchers spend a lifetime working towards the understanding of a specific complex problem and, as the culmination of their career, write a technical work offering such a profound and multilevel insight that it could not have been produced in any other way. Our contemporary lifestyle imposes enormous barriers against creating such life-career books, yet this is one. This extraordinary book provides incomparable understanding of piezoelectric materials and their behavior in electro-acoustic transducers.

Keywords: Ultrasonics, Piezoelectric, Transducers, Resonance, Piezoceramic, coupled fields, biparametric surfaces, stress state, strain state, piezoelectric bodies, defect, crack, acoustic impedance, amplitude characteristic, radial oscillation, analytical methods, dynamic model, electric impedance, electric field, stress intensity factor, frequent characteristic, longitudinal oscillations, numerical experiment, transversal oscillations, and biparametric visualization.

Dr. Ljubisa Peric, Author

COUPLED TENSORS OF PIEZOELECTRIC MATERIALS STATE AND APPLICATIONS

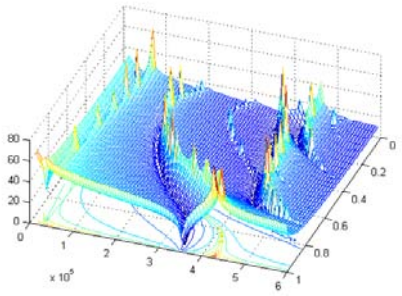

Published 2005 in Switzerland by MPI
430 pages,

Book can be ordered from:
MP Interconsulting
Marais 36
2400, Le Locle
Switzerland
mpi@bluewin.ch

Phone/Fax: +41- (0)-32-9314045
email:mpi@mpi-ultrasonics.com
http://www.mpi-ultrasonics.com
http://mastersonic.com

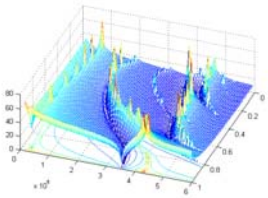

Dr. Ljubisa Peric,

COUPLED TENSORS OF PIEZOELECTRIC MATERIALS STATE AND APPLICATIONS

CONTENTS

List of Symbols

Universal Formula for Electric Impedance of Piezoelectric Ceramic Z_p

I have derived an **Universal Formula for Simulation of Electric Impedance Model** $Z_p = V / I\ [\Omega]$ of piezoelectric ceramic. Formula stands for all shapes of piezoelectric bodies: circular plate, circular-ring plate, rectangular plate, cylinder, circular-ring cylinder, circular-ring sectional cylinder, sphere, etc. Piezoceramic bodies may have *n*-th number of surfaces loaded by equal or different external loads: F_j^D or F_j^E (v_j^D or v_j^E - motion velocities of contour surfaces loaded by F_j^D or F_j^E) as interaction with outer medium, i.e., external mechanical impedances: Z_j^D or Z_j^E.

Formula enables precise determination of resonant frequencies of numerous radial, transversal, longitudinal, and lateral modes of oscillation even at design stage of piezoelectric transducers, and before manufacturing of piezoceramic elements and experimental measuring. Application field of piezo-sensors and actuators is very wide, and of special interest for **military industry** and **space research.** It may be also used for significant improvement of existing methods of modeling FEM, BEM, etc.

The formula is based on two constitutive system of equations:

Isothermal func. of internal energy $U(S_{ij}, D_i)$:	Isothermal func. of electric potential $H(S_{ij}, E_i)$:
$T_{rr}^D = c_{11}^D S_{rr} + c_{12}^D S_{\theta\theta} + c_{13}^D S_{zz} - h_{31} D_z,$	$T_{rr}^E = c_{11}^E S_{rr} + c_{12}^E S_{\theta\theta} + c_{13}^E S_{zz} - e_{31} E_z,$
$T_{\theta\theta}^D = c_{12}^D S_{rr} + c_{11}^D S_{\theta\theta} + c_{13}^D S_{zz} - h_{31} D_z,$	$T_{\theta\theta}^E = c_{12}^E S_{rr} + c_{11}^E S_{\theta\theta} + c_{13}^E S_{zz} - e_{31} E_z,$
$T_{zz}^D = c_{13}^D (S_{rr} + S_{\theta\theta}) + c_{33}^D S_{zz} - h_{33} D_z,$	$T_{zz}^E = c_{13}^E (S_{rr} + S_{\theta\theta}) + c_{33}^E S_{zz} - e_{33} E_z,$
$E_z^D = -h_{31} (S_{rr} + S_{\theta\theta}) - h_{33} S_{zz} + D_z / \varepsilon_{33}^S.$	$D_z^E = e_{31} (S_{rr} + S_{\theta\theta}) + e_{33} S_{zz} + \varepsilon_{33}^S E_z.$

Formula of electric impedance Z_p, for piezoelectric body with *n* surfaces is a function of numerous parameters.

Sum of all forms of energy in a conservative system is constant (First Law of Thermodynamics, or Law of Conservation of Energy):

$$\sum_{j=1}^{n-1} F_j^D v_j^D + V^D I = \sum_{j=1}^{n-1} F_j^E v_j^E + I^E V, \qquad n = 2, 3, 4, \ldots, k.$$

Then follows:

$$Z_p = \frac{V}{I} = \sqrt{\frac{z_{nn}^D + \sum_{i=1}^{n-1} z_{in}^D \bar{v}_i^D + \sum_{j=1}^{n-1} z_{nj}^D \bar{v}_j^D + \sum_{i=1}^{n-1}\sum_{j=1}^{n-1} z_{ij}^D \bar{v}_i^D \bar{v}_j^D}{z_{nn}^E + \sum_{i=1}^{n-1} z_{in}^E \bar{v}_i^E + \sum_{j=1}^{n-1} z_{nj}^E \bar{v}_j^E + \sum_{i=1}^{n-1}\sum_{j=1}^{n-1} z_{ij}^E \bar{v}_j^E \bar{v}_i^E}}, \qquad n = 2, 3, 4, \ldots, k.$$

z_{ij}^D, z_{nj}^D, z_{nn}^D, z_{ij}^E, z_{nj}^E and z_{nn}^E - internal mechanical and electric impedances, transfer functions of system (black box).

Comparison of derived formula by computer simulation using software package MATLAB, with analogous characteristic obtained by experimental measuring on Automatic Network Analyzer HP4194A, shows results at least 50% better than all known results published until now in scientific literature available to me.

Formula is applicable on: 1D, 2D, and 3D oscillating models of piezoelectric ceramic bodies, whose number of surfaces $S_n[m^2]$ may extend to infinity ($n \to \infty$). Also, it can join different assumed oscillation models (any combination of: 1D, 2D, and 3D model) of the same piezoceramic specimen loaded under equal conditions in the same period of time.

1 – Case: $n=2$ - **1D model** (transversal oscillation of the: circular plate, circular-ring plate, rectangular plate etc; or longitudinal oscillation of a: free beam, cantilever, cylinder, circular-ring cylinder, circular-ring sectional cylinder, etc.):

$$F_1^D v_1^D + V^D I = F_1^E v_1^E + I^E V,$$

$$Z_p = \frac{V}{I} = \sqrt{\frac{(z_{11}^D \bar{v}_1^D + z_{12}^D)\bar{v}_1^D + z_{21}^D \bar{v}_1^D + z_{22}^D}{(z_{11}^E \bar{v}_1^E + z_{12}^E)\bar{v}_1^E + z_{21}^E \bar{v}_1^E + z_{22}^E}}.$$

2 – Case: $n=3$ - **2D model** (radial oscillation of the: circular plate, circular-ring plate, rectangular plate, free beam, cantilever, cylinder, circular-ring cylinder, circular-ring sectional cylinder, etc.):

$$F_1^D v_1^D + F_2^D v_2^D + V^D I = F_1^E v_1^E + F_2^E v_2^E + I^E V,$$

$$Z_p = \frac{V}{I} = \sqrt{\frac{(z_{11}^D \bar{v}_1^D + z_{12}^D \bar{v}_2^D + z_{13}^D)\bar{v}_1^D + (z_{21}^D \bar{v}_1^D + z_{22}^D \bar{v}_2^D + z_{23}^D)\bar{v}_2^D + z_{31}^D \bar{v}_1^D + z_{32}^D \bar{v}_2^D + z_{33}^D}{(z_{11}^E \bar{v}_1^E + z_{12}^E \bar{v}_2^E + z_{13}^E)\bar{v}_1^E + (z_{21}^E \bar{v}_1^E + z_{22}^E \bar{v}_2^E + z_{23}^E)\bar{v}_2^E + z_{31}^E \bar{v}_1^E + z_{32}^E \bar{v}_2^E + z_{33}^E}}.$$

3 – Case: $n=4$ - **3D model** (3D oscillation of the: circular plate, circular-ring plate, rectangular plate, free beam, cantilever, cylinder, circular-ring cylinder, circular-ring sectional cylinder, etc.):

$$F_1^D v_1^D + F_2^D v_2^D + F_3^D v_3^D + V^D I = F_1^E v_1^E + F_2^E v_2^E + F_3^E v_3^E + I^E V,$$

$$Z_p = \frac{V}{I} = \sqrt{\frac{(z_{11}^D \bar{v}_1^D + z_{12}^D \bar{v}_2^D + z_{13}^D \bar{v}_3^D + z_{14}^D)\bar{v}_1^D + (z_{21}^D \bar{v}_1^D + z_{22}^D \bar{v}_2^D + z_{23}^D \bar{v}_3^D + z_{24}^D)\bar{v}_2^D + (z_{31}^D \bar{v}_1^D + z_{32}^D \bar{v}_2^D + z_{33}^D \bar{v}_3^D + z_{34}^D)\bar{v}_3^D + z_{41}^D \bar{v}_1^D + z_{42}^D \bar{v}_2^D + z_{43}^D \bar{v}_3^D + z_{44}^D}{(z_{11}^E \bar{v}_1^E + z_{12}^E \bar{v}_2^E + z_{13}^E \bar{v}_3^E + z_{14}^E)\bar{v}_1^E + (z_{21}^E \bar{v}_1^E + z_{22}^E \bar{v}_2^E + z_{23}^E \bar{v}_3^E + z_{24}^E)\bar{v}_2^E + (z_{31}^E \bar{v}_1^E + z_{32}^E \bar{v}_2^E + z_{33}^E \bar{v}_3^E + z_{34}^E)\bar{v}_3^E + z_{41}^E \bar{v}_1^E + z_{42}^E \bar{v}_2^E + z_{43}^E \bar{v}_3^E + z_{44}^E}}.$$

For PZT8 circular plate with dimensions: $2a_2 = 50\ [mm]$, $2h = 3[mm]$, $\rho = 7600[\frac{kg}{m^3}]$, whose coefficients are:

$c_{11}^E = 13{,}7 \cdot 10^{10}[N/m^2]$, $c_{12}^E = 6{,}97 \cdot 10^{10}$, $c_{13}^E = 7{,}16 \cdot 10^{10}$, $c_{33}^E = 12{,}4 \cdot 10^{10}$, $h_{31} = -7{,}8 \cdot 10^8 [V/m]$, $h_{33} = 26{,}9 \cdot 10^8 [V/m]$,
$c_{11}^D = 14 \cdot 10^{10}[\mathrm{N/m^2}]$, $c_{12}^D = 7{,}28 \cdot 10^{10}$, $c_{13}^D = 6{,}08 \cdot 10^{10}$, $c_{33}^D = 16{,}1 \cdot 10^{10}$, $e_{31} = -4[C/m^2]$, $e_{33} = 13{,}8$, $\varepsilon_{33}^S / \varepsilon_0 = 582$,

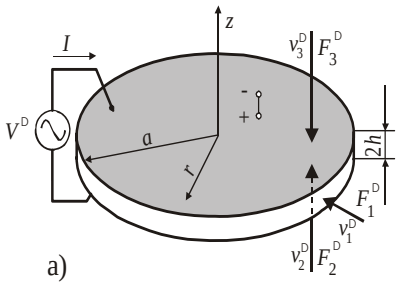

a)

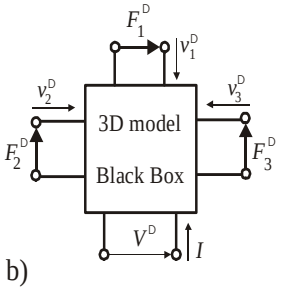

b)

$$\begin{Bmatrix} F_1^D \\ F_2^D \\ F_3^D \\ V^D \end{Bmatrix} = \begin{bmatrix} z_{11}^D & z_{12}^D & z_{13}^D & z_{14}^D \\ z_{21}^D & z_{22}^D & z_{23}^D & z_{24}^D \\ z_{31}^D & z_{32}^D & z_{33}^D & z_{34}^D \\ z_{41}^D & z_{42}^D & z_{43}^D & z_{44}^D \end{bmatrix} \begin{Bmatrix} v_1^D \\ v_2^D \\ v_3^D \\ I \end{Bmatrix}.$$

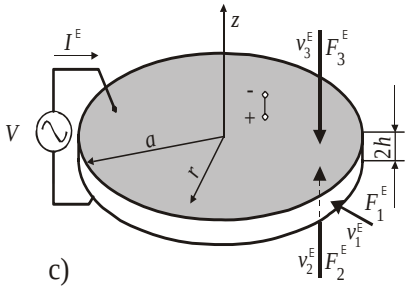

c)

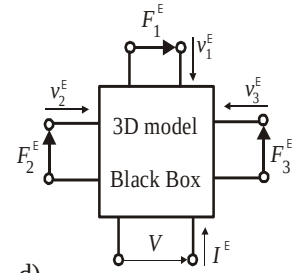

d)

$$\begin{Bmatrix} F_1^E \\ F_2^E \\ F_3^E \\ I^E \end{Bmatrix} = \begin{bmatrix} z_{11}^E & z_{12}^E & z_{13}^E & z_{14}^E \\ z_{21}^E & z_{22}^E & z_{23}^E & z_{24}^E \\ z_{31}^E & z_{32}^E & z_{33}^E & z_{34}^E \\ z_{41}^E & z_{42}^E & z_{43}^E & z_{44}^E \end{bmatrix} \begin{Bmatrix} v_1^E \\ v_2^E \\ v_3^E \\ V \end{Bmatrix}.$$

Formula provides following simulated characteristic of electric impedance model, which is compared with analogous, obtained by measuring on Automatic Network Analyzer HP4194A:

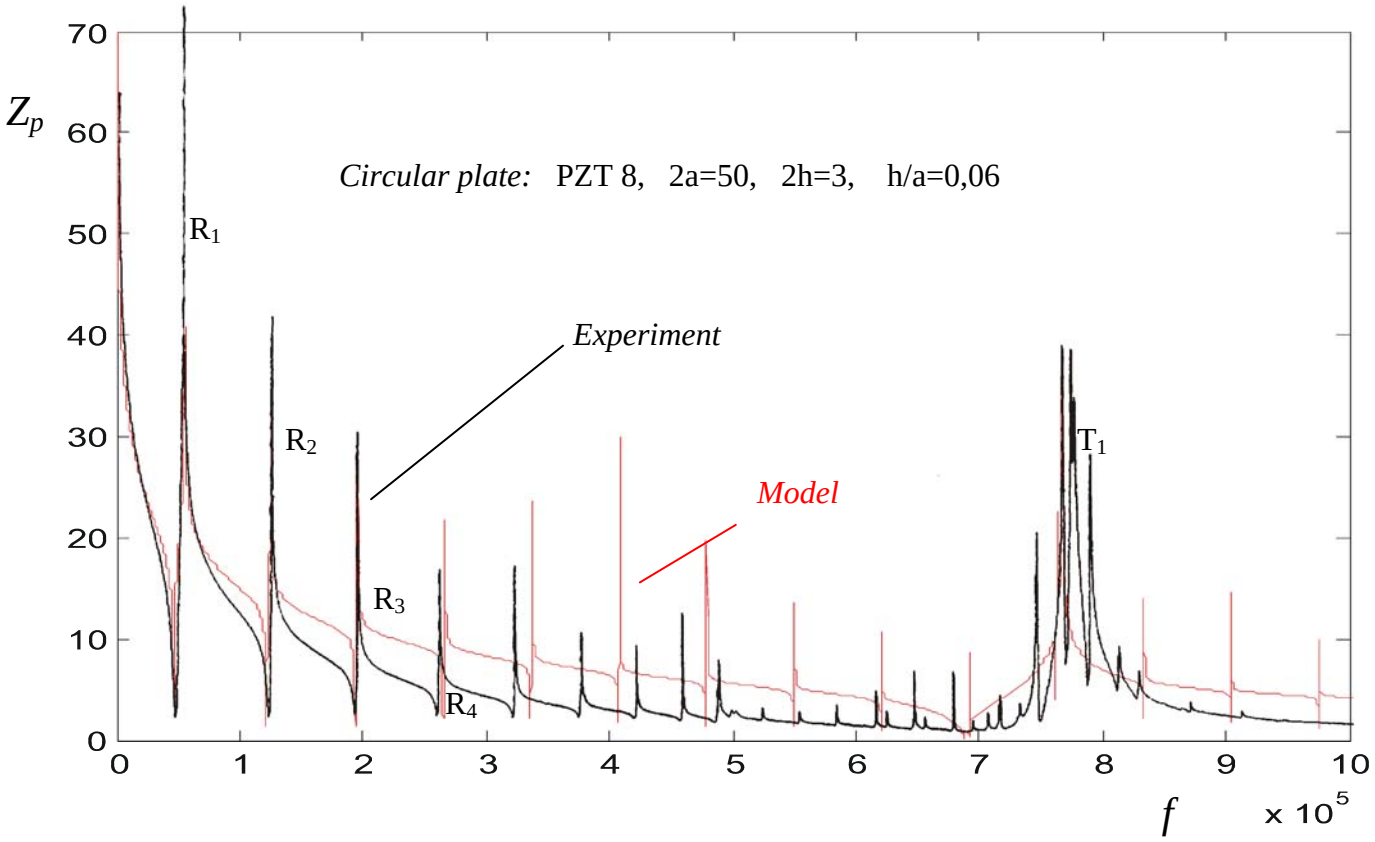

Knowing values of resonant frequencies is an initial condition during design of piezoceramic elements. From the picture above one may see that by this formula one may determine several exact positions of radial resonant modes R_1, R_2, R_3 and R_4, and transversal mode T_1, which are the most frequently used in technical practice and application.

4 – Case: $n=5$ - **3D model** (rectangular plate, free beam, etc.):

$$F_1^D v_1^D + F_2^D v_2^D + F_3^D v_3^D + F_4^D v_4^D + V^D I = F_1^E v_1^E + F_2^E v_2^E + F_3^E v_3^E + F_4^E v_4^E + I^E V,$$

$$Z_p = \frac{V}{I} = \sqrt{\frac{(z_{11}^D \bar{v}_1^D + z_{12}^D \bar{v}_2^D + z_{13}^D \bar{v}_3^D + z_{14}^D \bar{v}_4^D + z_{15}^D)\bar{v}_1^D + \ldots + (z_{41}^D \bar{v}_1^D + z_{42}^D \bar{v}_2^D + z_{43}^D \bar{v}_3^D + z_{44}^D \bar{v}_4^D + z_{45}^D)\bar{v}_4^D + z_{51}^D \bar{v}_1^D + z_{52}^D \bar{v}_2^D + z_{53}^D \bar{v}_3^D + z_{54}^D \bar{v}_4^D + z_{55}^D}{(z_{11}^E \bar{v}_1^E + z_{12}^E \bar{v}_2^E + z_{13}^E \bar{v}_3^E + z_{14}^E \bar{v}_4^E + z_{15}^E)\bar{v}_1^E + \ldots + (z_{41}^E \bar{v}_1^E + z_{42}^E \bar{v}_2^E + z_{43}^E \bar{v}_3^E + z_{44}^E \bar{v}_4^E + z_{45}^E)\bar{v}_4^E + z_{51}^E \bar{v}_1^E + z_{52}^E \bar{v}_2^E + z_{53}^E \bar{v}_3^E + z_{54}^E \bar{v}_4^E + z_{55}^E}}.$$

5 – Case: $n=6$ - **3D model** (rectangular plate with a circular or rectangular hole, etc.):

$$F_1^D v_1^D + F_2^D v_2^D + F_3^D v_3^D + F_4^D v_4^D + F_5^D v_5^D + V^D I = F_1^E v_1^E + F_2^E v_2^E + F_3^E v_3^E + F_4^E v_4^E + F_5^E v_5^E + I^E V,$$

$$Z_p = \frac{V}{I} = \sqrt{\frac{(z_{11}^D \bar{v}_1^D + z_{12}^D \bar{v}_2^D + z_{13}^D \bar{v}_3^D + z_{14}^D \bar{v}_4^D + z_{15}^D \bar{v}_5^D + z_{16}^D)\bar{v}_1^D + \ldots + (z_{51}^D \bar{v}_1^D + z_{52}^D \bar{v}_2^D + z_{53}^D \bar{v}_3^D + z_{54}^D \bar{v}_4^D + z_{55}^D \bar{v}_5^D + z_{56}^D)\bar{v}_6^D + z_{61}^D \bar{v}_1^D + z_{62}^D \bar{v}_2^D + z_{63}^D \bar{v}_3^D + z_{64}^D \bar{v}_4^D + z_{65}^D \bar{v}_5^D + z_{66}^D}{(z_{11}^E \bar{v}_1^E + z_{12}^E \bar{v}_2^E + z_{13}^E \bar{v}_3^E + z_{14}^E \bar{v}_4^E + z_{15}^E \bar{v}_5^E + z_{16}^E)\bar{v}_1^E + \ldots + (z_{51}^E \bar{v}_1^E + z_{52}^E \bar{v}_2^E + z_{53}^E \bar{v}_3^E + z_{54}^E \bar{v}_4^E + z_{55}^E \bar{v}_5^E + z_{56}^E)\bar{v}_6^E + z_{61}^E \bar{v}_1^E + z_{62}^E \bar{v}_2^E + z_{63}^E \bar{v}_3^E + z_{64}^E \bar{v}_4^E + z_{65}^E \bar{v}_5^E + z_{66}^E}}.$$

…, etc.

8.5.4. Second Approach to 3D Problem of Oscillations of Circular-ring Plate

In this part of the paper are considered 3D spatial oscillations of circular-ring plate with electrode coatings and transversal polarization along axis z Figure 8.121 – a. 3D model by which can be described spatial oscillation of piezoceramic circular-ring plate, may be presented using the black box analogy, Figure 8.121 – b.

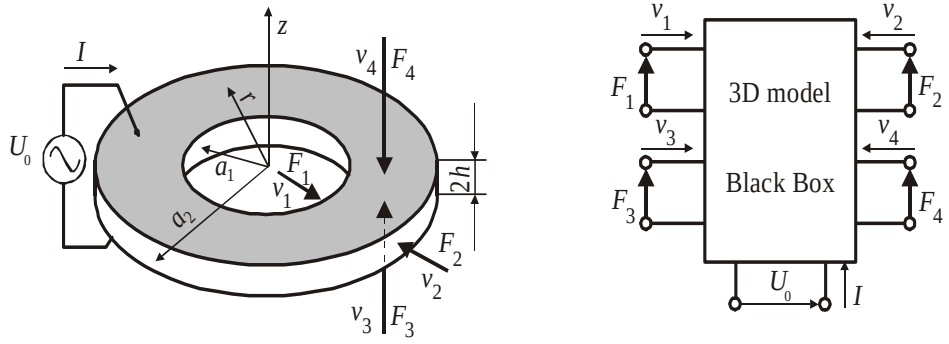

a) b)

Figure 8.121. – *3D model of circular-ring plate*

It may be seen that *circular-ring plate* may be observed as *black box* device with five variable parameters (five input-output values). First group of values (usually used as input – leading of electric energy on plate coatings from electric generator of alternate voltage) is *electric voltage* U_0 and *electric current strength I*. Remained four groups of values conform to cylindric surfaces - $r = a_1$ (*surface force* F_1 and *velocity* v_1), $r = a_2$ (*surface force* F_2 and *velocity* v_2), and plane mutually opposite surfaces $z = -h$ (*surface force* F_3 and *velocity* v_3), and $z = h$ (*surface force* F_4 and *velocity* v_4).

Oscillations of circular-ring plate are excited by leading of alternate difference of electric potential $2U_0 e^{i\omega t}$ on surfaces $z = \pm h$. *Plate oscillations*, i.e., *vibration of particles*, have *radial-transversal character of motion*, that is $\vec{s} = u(r,\ t)\vec{r}_0 + w(z,\ t)\vec{k}$.

Equations of piezoelectric effect, which are used in this analysis and procedure of derivation is identical with procedure in item 8.5.2♣, expressions (8.271) ÷ (8.275).

Partial differential equations of oscillation of circular-ring plate:

$$c_{11}^D\left(\frac{\partial^2 u}{\partial r^2} + \frac{1}{r}\frac{\partial u}{\partial r} - \frac{u}{r^2}\right) = \rho\frac{\partial^2 u}{\partial t^2},$$

$$c_{33}^D\frac{\partial^2 w}{\partial z^2} = \rho\frac{\partial^2 w}{\partial t^2} \qquad (8.321)$$

♣ 8.5.1. 3D model of oscillations of circular plate

8.5.5.1. *Diagrams of Spatial States*

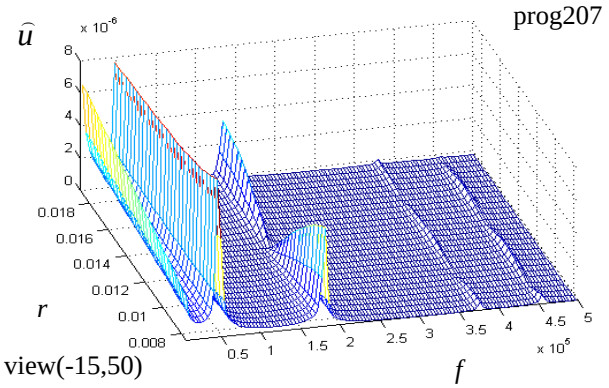

Figure 8.122. – *Componential displacement* $\hat{u} = \hat{u}(f, r)$

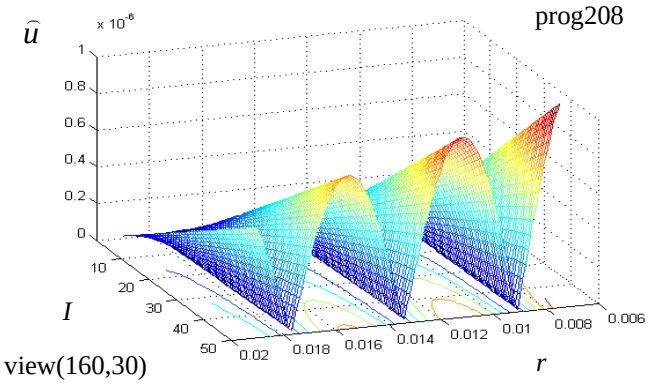

Figure 8.123. – *Componential displacement* $\hat{u} = \hat{u}(r, I)$

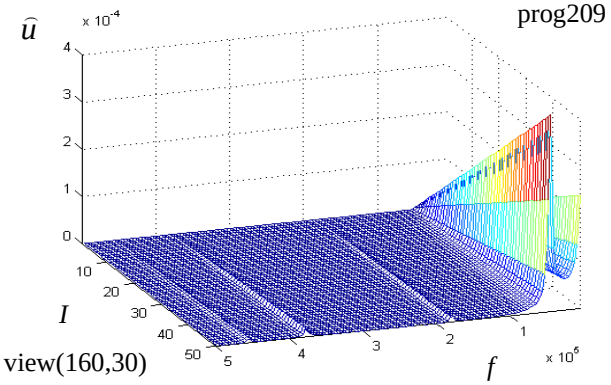

Figure 8.124. – *Componential displacement* $\hat{u} = \hat{u}(f, I)$

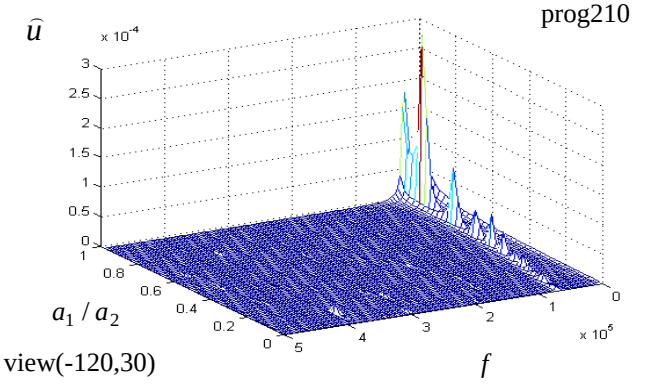

Fig. 8.125. – *Component. Displacement* $\hat{u} = \hat{u}(f, a_1 / a_2)$

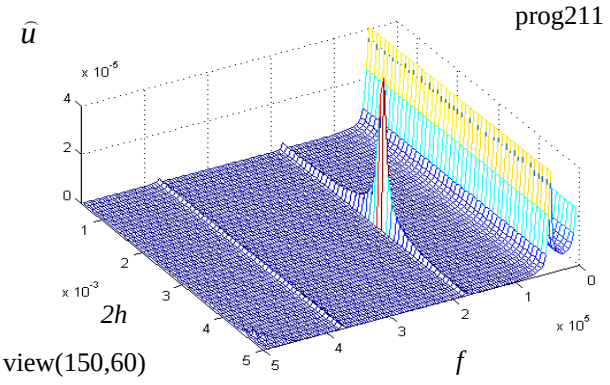

Figure 8.126. – *Componential displacement* $\hat{u} = \hat{u}(f, 2h)$

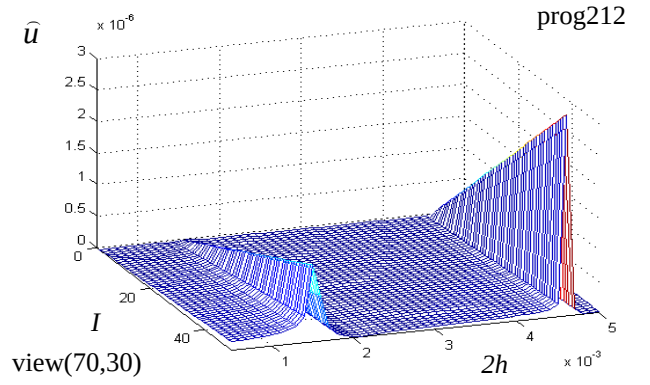

Figure 8.127. – *Componential displacement* $\hat{u} = \hat{u}(I, 2h)$

I

r

view(120,60) $2h$ a_1 / a_2

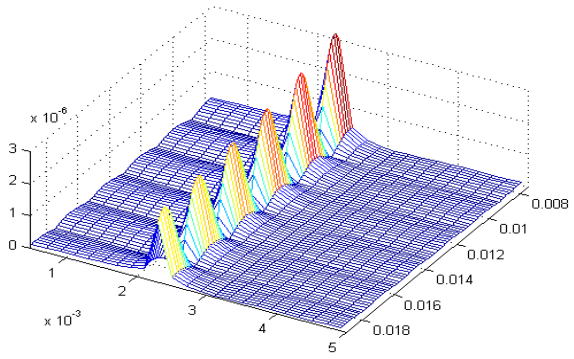

Figure 8.128. – *Componential displacement* $\widehat{u} = \widehat{u}(r, 2h)$

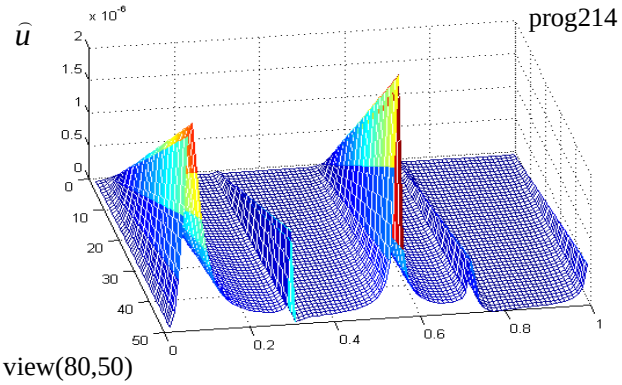

Fig. 8.129. – *Component. Displacement* $\widehat{u} = \widehat{u}(I,\ a_1 / a_2)$

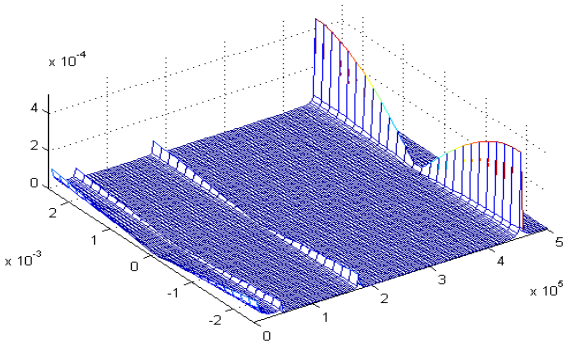

Figure 8.130. – *Componential displacement* $\widehat{w} = \widehat{w}(f,\ z)$

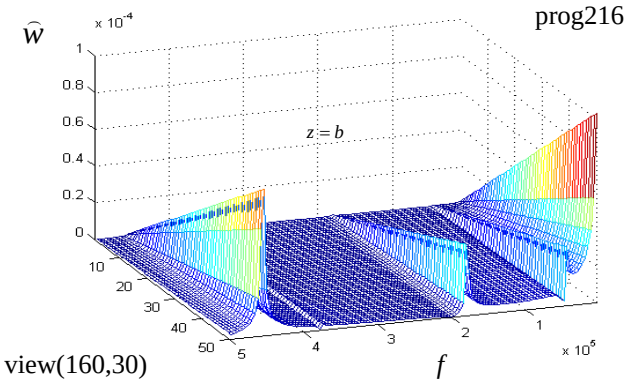

Figure 8.131. – *Componential displacement* $\widehat{w} = \widehat{w}(f,\ I)$

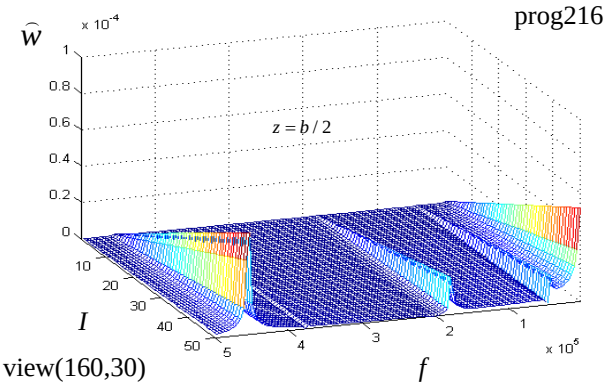

Figure 8.132. – *Componential displacement* $\widehat{w} = \widehat{w}(f,\ I)$

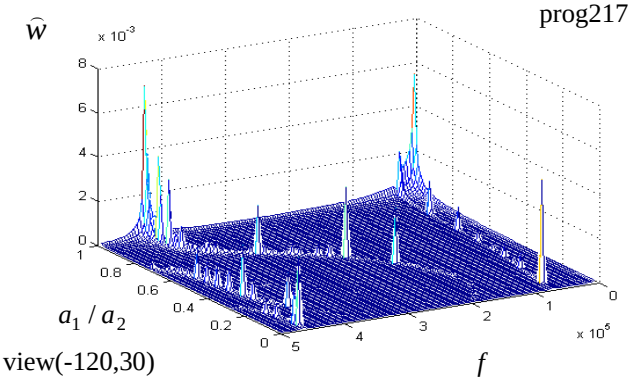

Fig. 8.133. – *Component. Displacement* $\widehat{w} = \widehat{w}(f,\ a_1/a_2)$

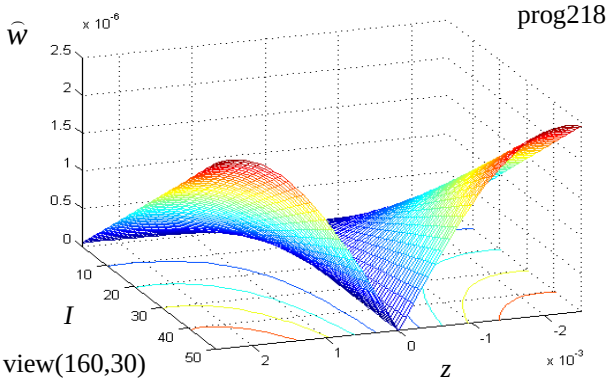

Figure 8.134. – *Componential displacement* $\widehat{w} = \widehat{w}(z,\ I)$

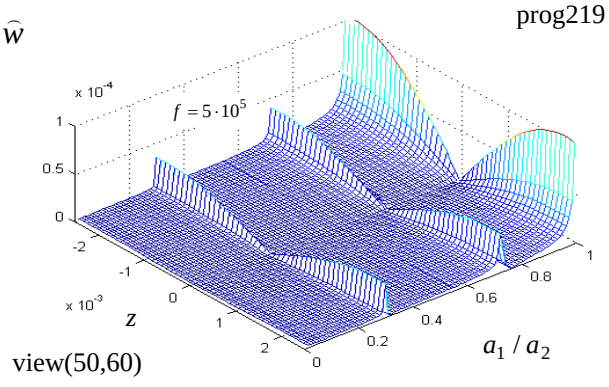

Fig. 8.135. – *Component. Displacement* $\widehat{w} = \widehat{w}(z,\ a_1 / a_2)$

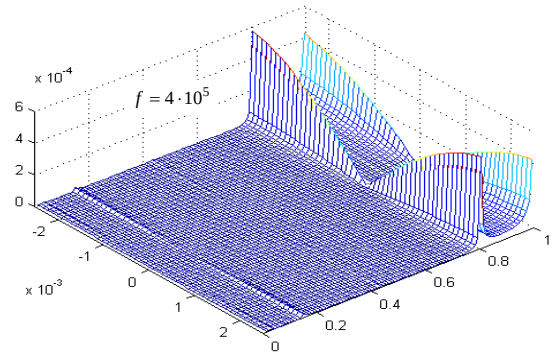

Fif. 8.136. – *Component. Displacement* $\hat{w} = \hat{w}(z, a_1 / a_2)$

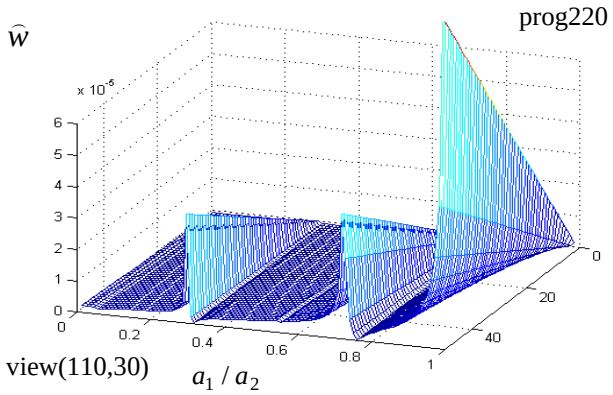

Fif. 8.137. – *Component. Displacement* $\hat{w} = \hat{w}(I, a_1 / a_2)$

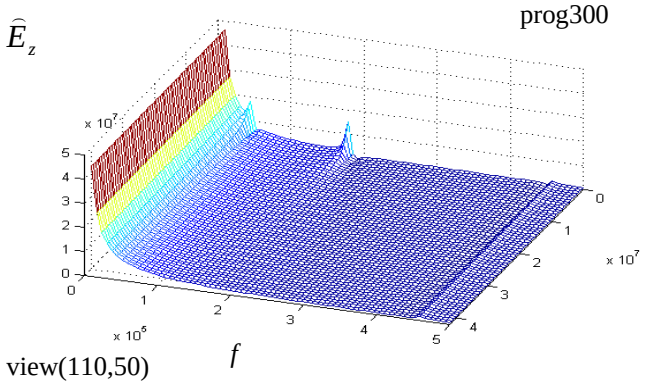

Fif. 8.274. – *Electric field* $\hat{E}_z = \hat{E}_z(f, Z_1 / Z_2)$

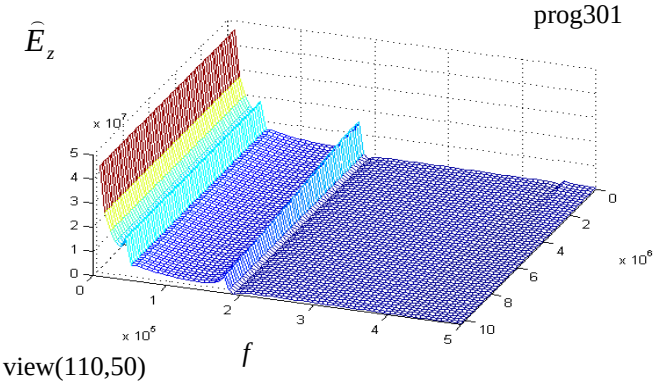

Fif. 8.275. – *Electric field* $\hat{E}_z = \hat{E}_z(f, Z_3 / Z_4)$

In order to show the possibility of analysis of piezoceramic circular-ring elements of concrete dimensions, a numerical analysis of the proposed model $Z_{ul} = Z_{ul}(f)$ is performed, using software package MATLAB. Concretely, an input electric impedance is determined for PZT8 piezoceramic circular-ring plate (Figure 8.276, programme 200 – Appendix III), whose tensors of material coefficients are given in Appendix II, with dimensions $2a_2 = 38[mm]$, $2a_1 = 15[mm]$, and $2h = 5[mm]$. It is assumed that all contour surfaces of circular-ring plate oscillate freely in air without additional external loading.

Comparison of obtained input electric impedance from Figure 8.276. is performed with analogous characteristic obtained by standard *Mason's* transversal (crossing) one-dimensional model [306] (Figure 8.277). One may notice that for the *first transversal mode* (T_1) exists satisfactory coincidence of both models. Small deviations that exist are result of coupled effect of action between transversal and radial mode of oscillation at adopted 3D model. Further, one may notice that one-dimensional *Mason's model* does not encompass radial resonant modes (R_1, R_2, R_3, R_4), which presents the proposed 3D model.

On Figure 8.278. is presented *comparative characteristic* of input electric impedance of adopted 3D model with characteristic of radial two-dimensional model [222]. One may notice that for the first two radial resonant modes of oscillation (R_1, R_2), exists good agreement, while for the rest radial resonant modes is characteristic deviation due to the great effect of transversal resonant mode at proposed 3D model. From Figure 8.278. one may notice that *two-dimensional radial model* cannot present *transversal mode of oscillation* (T_1).

On Figure 8.279. is presented comparison of electric impedance characteristics of adopted 3D model with 3D model proposed by *Brissaud* [53, 54]. One may notice that *Brissaud's model* contains certain limits and faults. Good coincidence is only at the first radial resonant mode (R_1), while at remained radial resonant modes deviations are significant. Also is illogical phenomenon at radial mode R_4 (*Brissaud's model*), that *characteristic of electric impedance* gets maximum first, and then minimum (region marked with arrow), which is not feasible and real. Beside the quoted faults of *Brissaud's* 3D model, one more is noticed, that it cannot encompass effect of external mechanical loads on boundary contour surfaces of circular-ring piezoceramic plate. Cited facts confirm great advantage of the proposed 3D model,[♣] which is detailedly analyzed and derived in previous item (8.5.4).

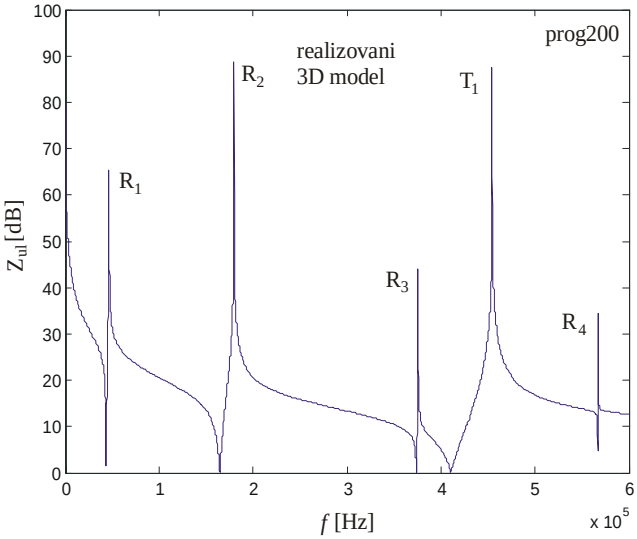

Figure 8.276. - *Electric impedance* $Z_{ul} = Z_{ul}(f)$

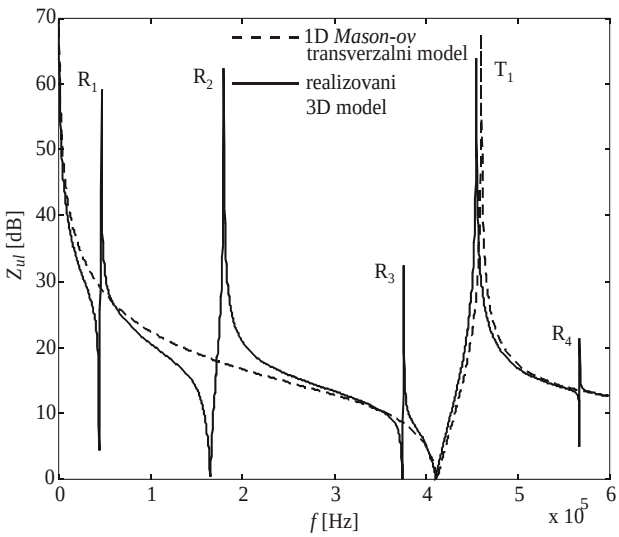

Figure 8.277. - *Electric impedance* $Z_{ul} = Z_{ul}(f)$

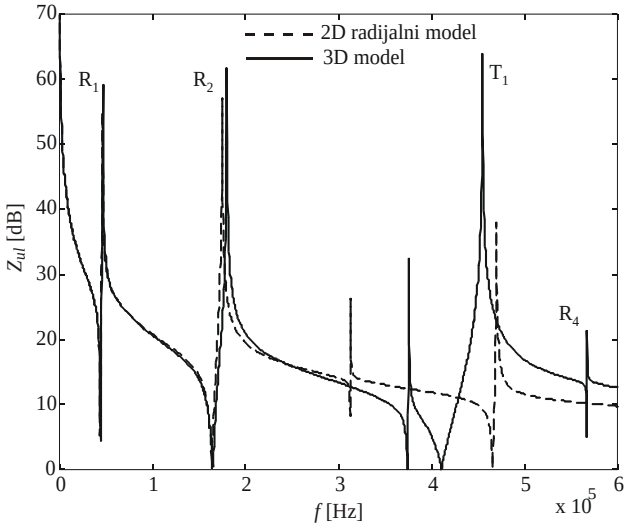

Figure 8.278. - *Electric impedance* $Z_{ul} = Z_{ul}(f)$

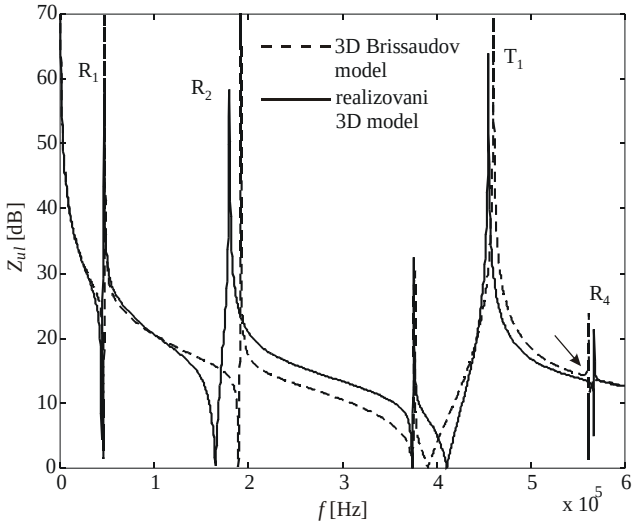

Figure 8.279. - *Electric impedance* $Z_{ul} = Z_{ul}(f)$

[♣] 8.5.4. Second approach to the problem of 3D oscillations of circularring plate.

On Figure 8.280. is presented *characteristic of electric impedance dependence of frequency* for the same PZT8 piezoceramic specimen, thereat now are contour surfaces of the circular-ring plate loaded with different external loads (different acoustic impedances). Solid line represents case of piezoceramic circular-ring plate that oscillates freely in air without additional external load. Dashed line represents case when top metalized surface of the circular-ring plate $(z = h)$ is loaded, while other surfaces are free. Dotted line is case of simultaneous loading of both top and bottom metalized surface $z = \pm h$. From Figure 8.280 one may see that *acoustic load* of the circular-ring plate in transversal direction affects mostly the transversal (crossing) mode of oscillation, while its influence on radial modes may be neglected.

On Figure 8.281. is presented case of loading of cylindric contour surfaces of circular-ring plate in radial direction. One may notice that increase of acoustic load in radial direction considerably affects radial resonant modes of oscillation of circular-ring plate, while influence on transversal modes may be neglected. Solid line represents *circular-ring plate* that oscillates freely in air without additional external load. Dashed line represents action of acoustic load on internal cylindric surface $r = a_1$, and dotted line simultaneous action of acoustic load on internal and external cylindric surface $(r = a_1$ and $r = a_2)$.

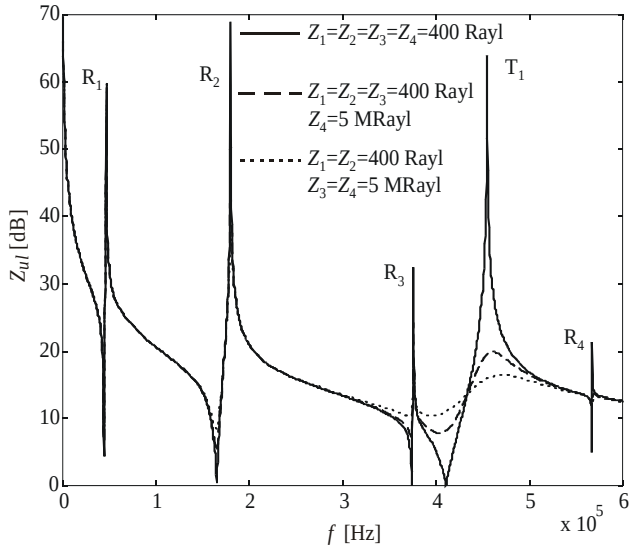

Figure 8.280. - *Electric impedance* $Z_{ul} = Z_{ul}(f)$

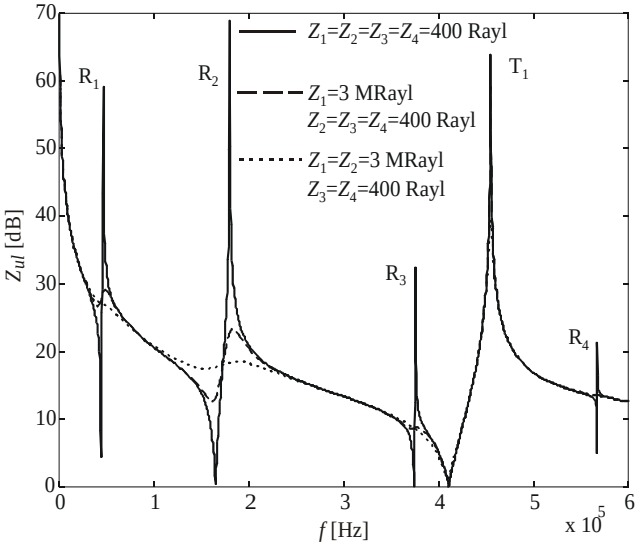

Figure 8.281. - *Electric impedance* $Z_{ul} = Z_{ul}(f)$

In order to further represent capabilities of proposed 3D model on Figure 8.282. and 8.283., *dependence of electric impedance in function of frequency f* and thickness of the ring *2h* is presented.

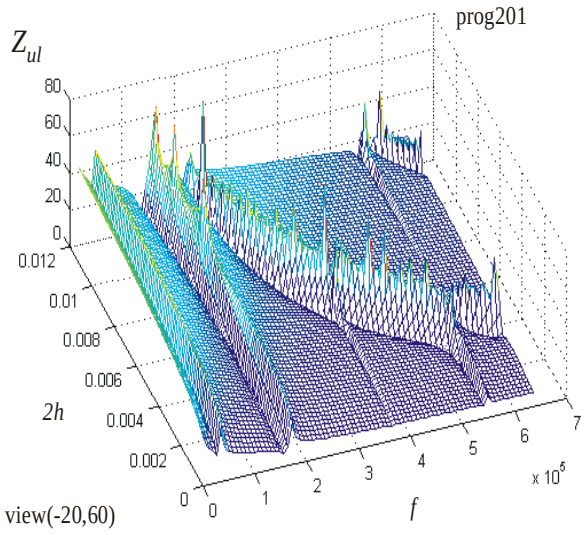

Figure 8.282. - *Electric impedance* $Z_{ul} = Z_{ul}(f,\ 2h)$

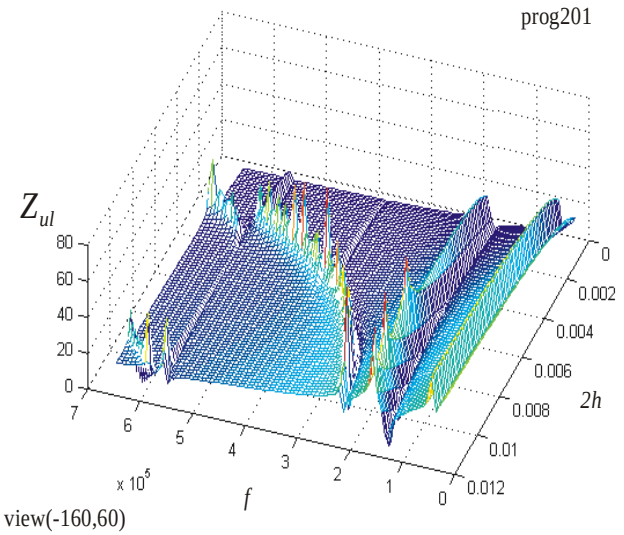

Figure 8.283. - *Electric impedance* $Z_{ul} = Z_{ul}(f,\ 2h)$

It is adopted that thickness of the circular-ring plate is in range $2h = 0 \div 12\ mm$. From Figure 8.282. one may notice that increase of the ring thickness affects mostly the *transversal (crossing) resonant mode* of oscillation, which shifts to the region of lower frequencies, and less the radial resonant normal modes of oscillation. *Radial resonant modes* shift too, but it is a result of mutual coupling with transversal resonant mode of oscillation. Also, change of thickness of circular-ring plate affects *value of capacitance of piezoceramic ring*, which reflects on the change of level height of electric impedance (Figure 8.282 and Figure 8.283).

On Figure 8.284. and 8.285. is presented *input electric impedance* Z_{ul} in function of frequency *f* and ratio of internal and external radius a_1 / a_2 (range is $a_1 / a_2 = 0 \div 1$).

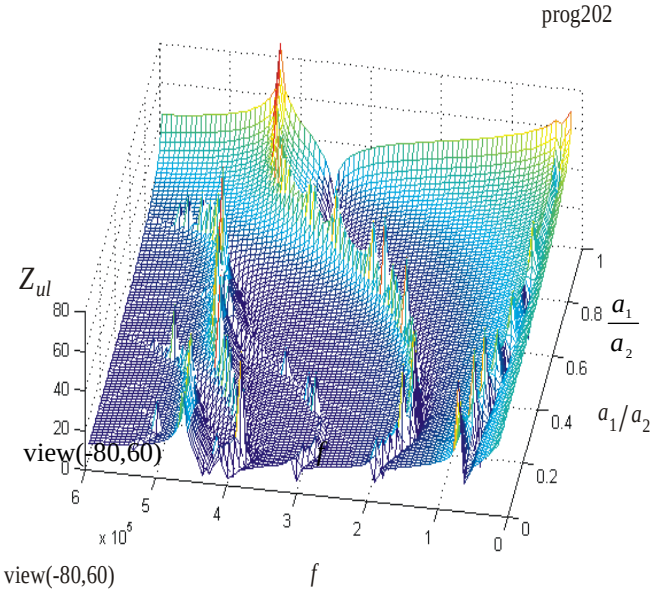

Figure 8.284. - *Electric impedance* $Z_{ul} = Z_{ul}(f,\ a_1 / a_2)$

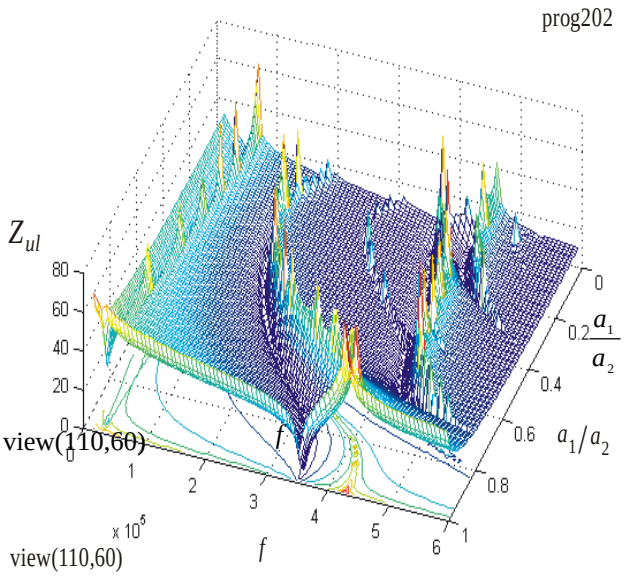

Figure 8.285. - *Electric impedance* $Z_{ul} = Z_{ul}(f,\ a_1 / a_2)$

As expected, one may see (Figure 8.284. and Figure 8.285) that change of radius ratio has the greatest influence on state of radial resonant modes, thereat one may notice an interesting phenomenon that first *radial resonant mode* moves to lower frequencies, while other radial resonant modes tend to higher frequencies, and thereat considerably affect the *transversal resonant mode*. This influence of internal radius on resonant frequency of transversal oscillations was not analyzed till now in the field of modelling of piezoceramic circular-ring plates and ultrasonic sandwich transducers. Similarly to the previous case, alteration of area size of metalized surface due to the alteration of internal radius generates alteration of its capacitance, and by itself also change of level value of input electric impedance.

Results from previous analysis can be presented more clearly through diagrams of spatial states of input electric impedance Z_{ul} in function of frequency and applied external load (applied acoustic impedance) Z_3 and Z_4. Spatial diagrams of input electric impedance presented on Figure 8.286. and 8.287 conform to the input electric impedance from Figure 8.280., while spatial diagrams of input electric impedance presented on Figure 8.288. and 8.289 conform to the input electric impedance from Figure 8.281. On these Figures are clearly noticed values of external (acoustic) loads at which some *resonant modes* disappear.

Transversal (crossing) mode of oscillation disappears with increase of external load in direction of polarization axis across thickness of circular-ring plate (Figure 8.286. and Figure 8.287). Radial mode of oscillation disappears with increase of acoustic load Z_1 and Z_2 in radial direction on cylindric surfaces of circular-ring plate (Figure 8.288. and Figure 8.289). However, since it is about coupled tensors of state, these influences are not isolated (independent), but also the *resonant modes are coupled*. From Figure 8.286. and 8.287. One may see that changes at transversal resonant mode also affect changes of the third and fourth radial mode of oscillation, which are closest to the transversal mode, and at high external loads they also affect changes of distant radial resonant mode of oscillation.

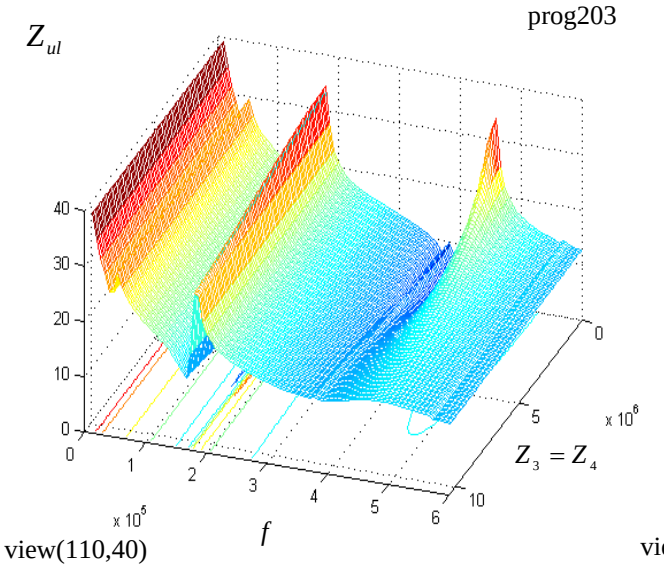

Fig. 8.286. - *Electric impedance* $Z_{ul} = Z_{ul}(f,\ Z_3 = Z_4)$

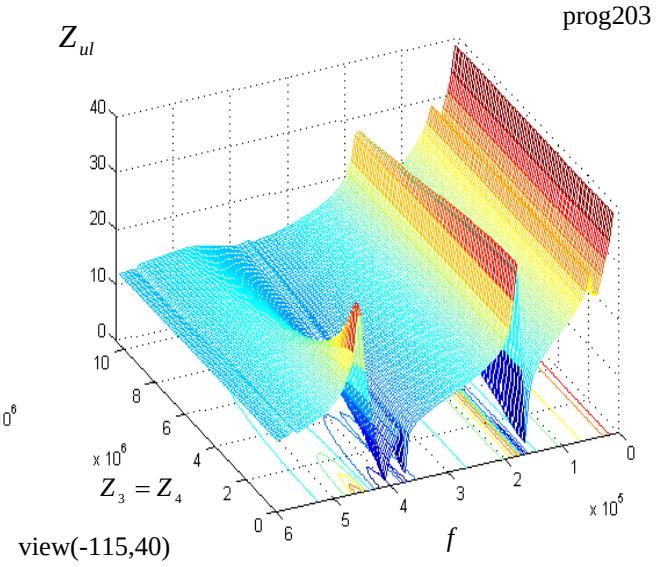

Fig. 8.287. - *Electric impedance* $Z_{ul} = Z_{ul}(f,\ Z_3 = Z_4)$

prog204

Z_{ul}

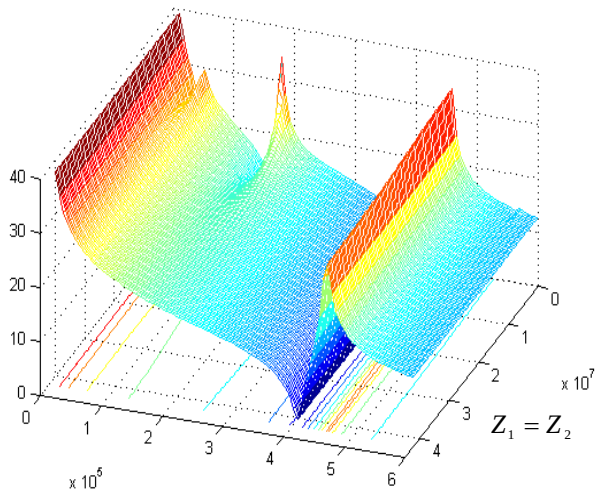

view(110,40)

Fig. 8.288. - *Electric impedance* $Z_{ul} = Z_{ul}(f,\ Z_1 = Z_2)$

prog204

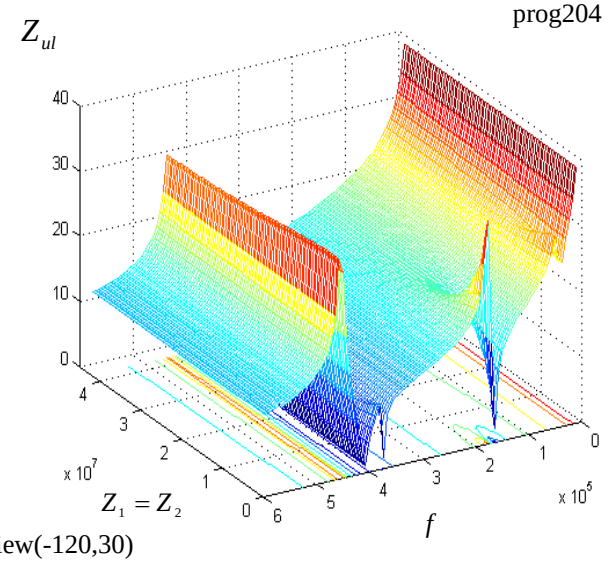

view(-120,30)

Fig. 8.289. - *Electric impedance* $Z_{ul} = Z_{ul}(f,\ Z_1 = Z_2)$

Mutual arrangement of radial and transversal resonant modes of oscillation depend of relation between internal and external radius, as well as of thickness of the piezoceramic circular-ring plate itself (figures 8.282, 8.283, 8.284, and 8.285). For definite concrete dimensions of piezoceramic circular-ring plate *resonant modes of oscillation* may be very close, and analyzed mechanical external load caused by acoustic impedances, can generate, besides intensity decrease of resonant modes, also their frequency *shift*. So, for example, at circular-ring plate with small external diameter and greater height, cylindric lateral surfaces become dominant, and lateral external radial loads (acoustic impedances) have significant influence on radial resonant modes of oscillation. In these cases, disappearing of radial modes with increase of external load can generate *frequency shift* of transversal mode of oscillation because of their very significant mutual coupling (*coupled tensors of piezoelectric material state*).

8.5.5.2. *Analysis of Numerical and Experimental Results*

Main task was to obtain experimental verification of adopted and analyzed 3D model[♣] for coupled tensors of state of piezoelectric materials, what was the ultimate goal of this dissertation. *Input electric impedance* in function of frequency $Z_{ul} = Z_{ul}(f)$ is measured for different piezoceramic elements in shape of circular-ring plates and circular plates. Obtained experimental results are compared with correspondent results for adopted model obtained by using of software package MATLAB (Figure 8.290). In experimental and numerical analysis are used two types of piezoceramic materials, PZT4 and PZT8, whose tensors *of material coefficients* are presented in Appendix II. Here are observed cases of oscillation of piezoceramic specimens by excitation, i.e., by leading of electric energy from alternate voltage generator on electrode coatings that are located on principal mutually parallel plane surfaces, and which are perpendicular to the axis of polarization (Figure 8.121). In Appendix III are presented *characteristic programmes of numerical analysis using software package* MATLAB for *proposed and analyzed model* of circular-ring plate from Figure 8.121, and that is an *universal* 3D *model*, because it very well numerically simulates mutually coupled tensors at piezoceramic circular-ring plates and circular plates, as in plane,

[♣] 8.5.4. Second approach to the problem of 3D oscillations of circular-ring plate.

so in space. Other programmes used in this dissertation are similar, and they are not presented because of volume and complexity of exposed matter. Dependence of electric impedance of frequency, for piezoceramic circular-ring plates and circular plates, is experimentally measured by *automatic network analyzer* HP4194A♣, and comparative results are presented on Figures 8.291, 8.293, 8.295, 8.297, 8.299, 8.301.

On Figure 8.290. is presented *characteristic of modulus of input electric impedance, simulated numerically on computer* in function of frequency, for PZT8 piezoceramic circular-ring plate with dimensions $2a_1 = 4\,[mm]$, $2a_2 = 10\,[mm]$, and $2h = 2\,[mm]$. It is assumed that oscillation is performed in air without additional external loading.

On Figure 8.291. is presented comparison of quoted numerically simulated and measured experimental dependence of modulus of input electric impedance.

From Figure 8.290. and 8.291. one may see that forms and calculated values of input electric impedances, as well as calculated values of resonant and antiresonant frequency of oscillation for circular-ring piezoceramic plate, are very close to the correspondent experimentally obtained results, as for the *first radial mode of oscillation* R_1, as well as for the *first transversal (crossing) mode of* oscillation T_1.

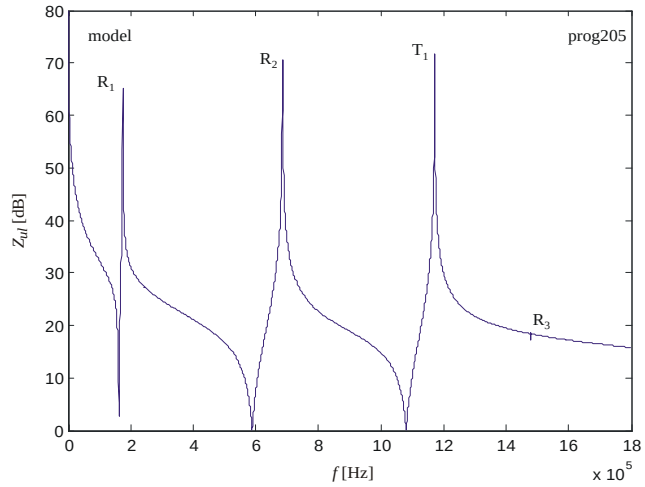

Figure 8.290. - *Electric impedance* $Z_{ul} = Z_{ul}(f)$

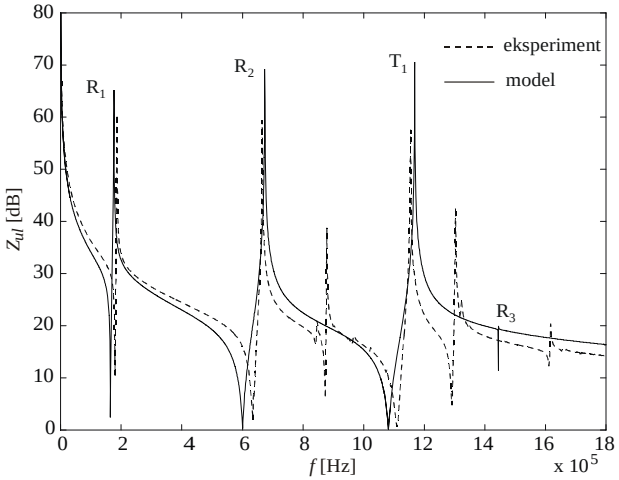

Figure 8.291. - *Electric impedance* $Z_{ul} = Z_{ul}(f)$

On Figure 8.292. is presented *characteristic of modulus of input electric impedance, simulated numerically on computer* in function of frequency, for PZT4 piezoceramic circular-ring plate with dimensions $2a_1 = 13\,[mm]$, $2a_2 = 38\,[mm]$, and $2h = 4\,[mm]$. It is assumed that oscillation is performed in air without additional external loading.

On Figure 8.293. is presented comparison of *characteristic* of modulus of input electric impedance *numerically simulated on computer,* and *experimental characteristic measured* on automatic network analyzer HP4194A.

♣ Network Impedance Analyzer.

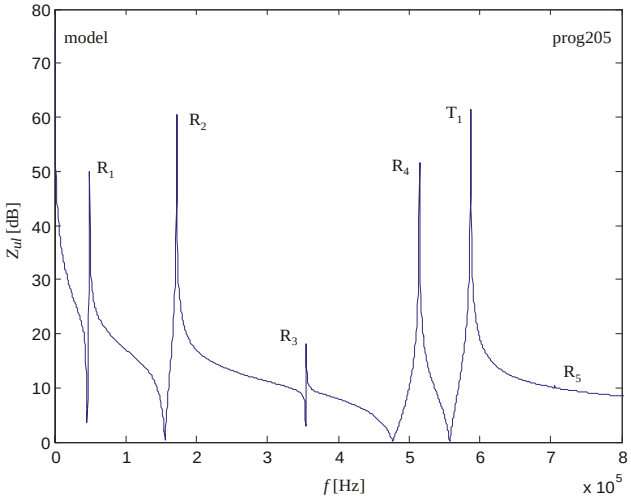

Figure 8.292. - *Electric impedance* $Z_{ul} = Z_{ul}(f)$

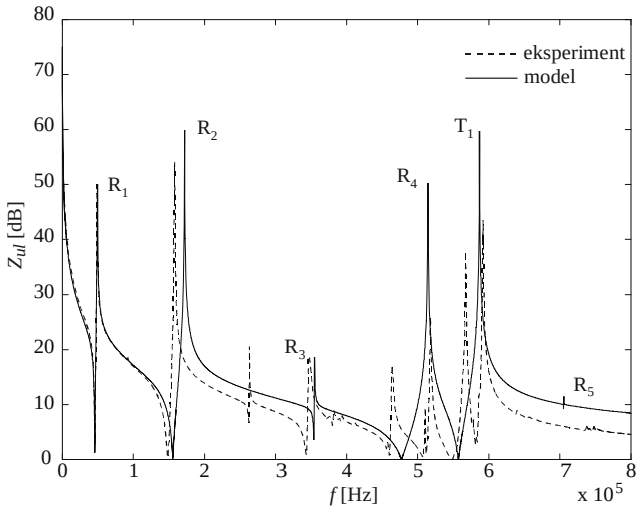

Figure 8.293. - *Electric impedance* $Z_{ul} = Z_{ul}(f)$

On Figure 8.294. is presented *characteristic of modulus of input electric impedance, simulated numerically on computer* in function of frequency, for PZT4 piezoceramic circular-ring plate with dimensions $2a_1 = 13\,[mm]$, $2a_2 = 38\,[mm]$, and $2h = 6{,}35\,[mm]$. It is assumed that oscillation is performed in air without additional external loading.

On Figure 8.295 is presented comparison of simulated and experimentally measured dependence of modulus of input electric impedance.

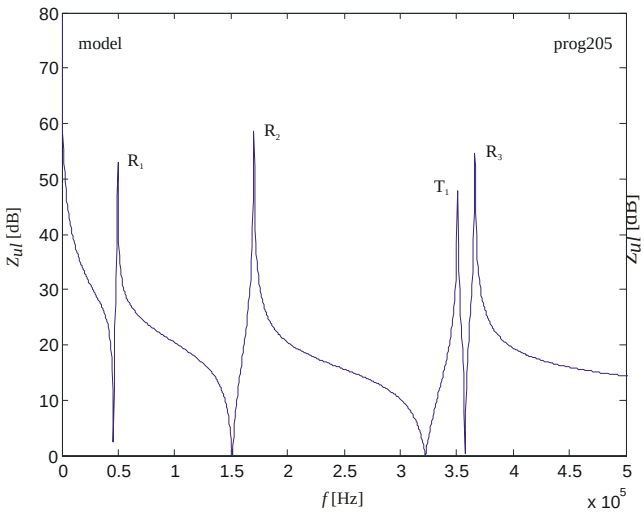

Figure 8.294. - *Electric impedance* $Z_{ul} = Z_{ul}(f)$

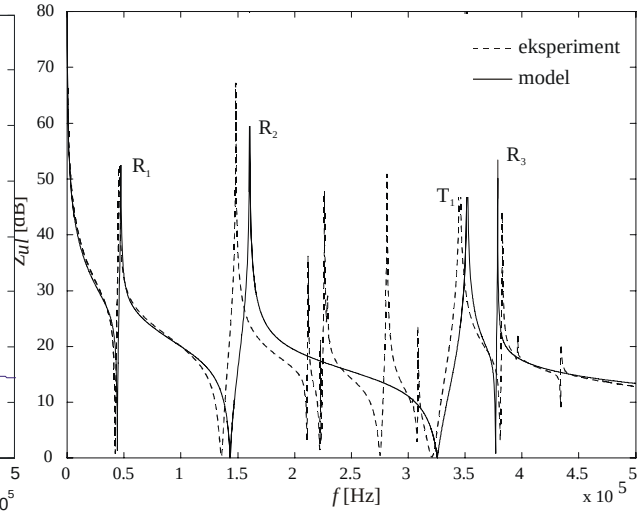

Figure 8.295. - *Electric impedance* $Z_{ul} = Z_{ul}(f)$

First radial mode R_1 and *first transversal mode* T_1 are the most often-used modes of oscillation at piezoelectric transducers in practical application. Adopted and analyzed model, as one may see, predicts with very good accuracy these modes of oscillation at different types of piezoceramic circular-ring specimens. *Transversal mode of oscillation* T_1 is most frequently used at ultrasonic high frequency

transducers. However, there is often need in practice for use of transducers at lower frequencies. Obtaining of lower operating resonant frequencies is possible to realize by application of *Langevin's* sandwich transducer, or simple piezoceramic circular-ring plate (or circular plate), which oscillates in its first radial mode R_1. At first radial resonant mode R_1 a considerable stressing in transversal (crossing) direction exists because of the elastic coupling and high interaction between coupled *tensors of state of piezoelectric materials*. Analysis of the cited transversal oscillation of circular-ring piezoceramic plate is enabled by proposed 3D model, and it may be broadened on cylindric piezoceramic bodies in shape of circular plates. Adopted 3D model considers mutual coupling of transversal and radial oscillations, and thereby is possible to determine optimal geometry of circular-ring plate or circular plate, in order to obtain increased displacement in transversal direction during oscillation in region of the first radial mode.

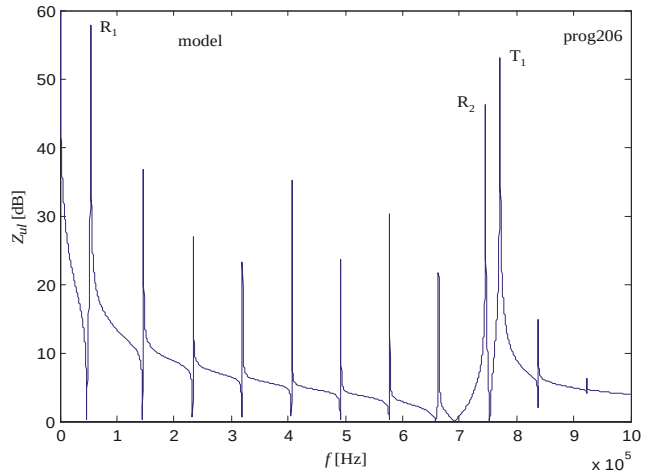

Figure 8.296. - *Electric impedance* $Z_{ul} = Z_{ul}(f)$

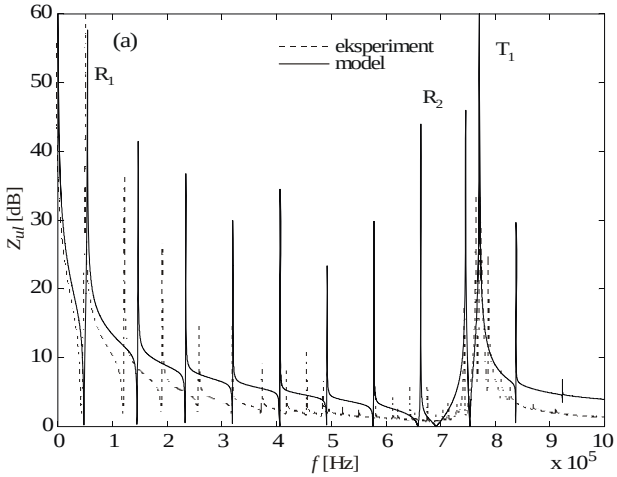

Figure 8.297. - *Electric impedance* $Z_{ul} = Z_{ul}(f)$

On Figure 8.296. is presented *characteristic of modulus of input electric impedance, simulated numerically on computer* in function of frequency, for PZT8 piezoceramic circular plate with dimensions $2a_2 = 50\,[mm]$, and $2h = 3\,[mm]$. It is assumed that oscillation is performed in air without additional external loading. On Figure 8.297. is presented comparison of numerically simulated and experimentally measured dependence of modulus of input electric impedance.

On Figure 8.298. is presented *characteristic of modulus of input electric impedance, simulated numerically on computer* in function of frequency, for PZT4 piezoceramic circular plate with dimensions $2a_2 = 20\,[mm]$, i $2h = 5\,[mm]$. It is assumed that oscillation is performed in air without additional external loading. On Figure 8.299. is presented comparison of numerically simulated and experimentally measured dependence of modulus of input electric impedance.

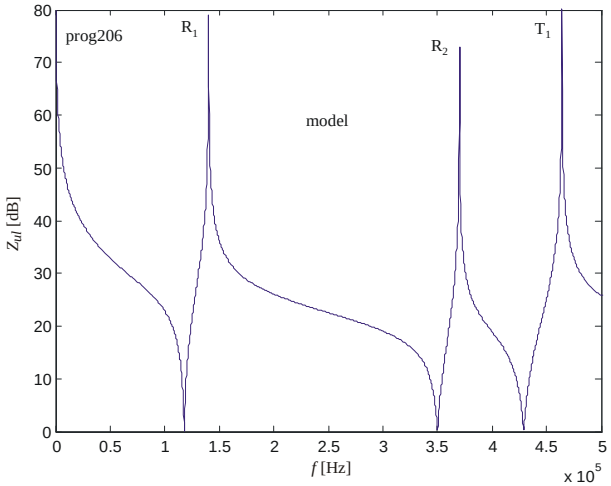

Figure 8.298. - *Electric impedance* $Z_{ul} = Z_{ul}(f)$

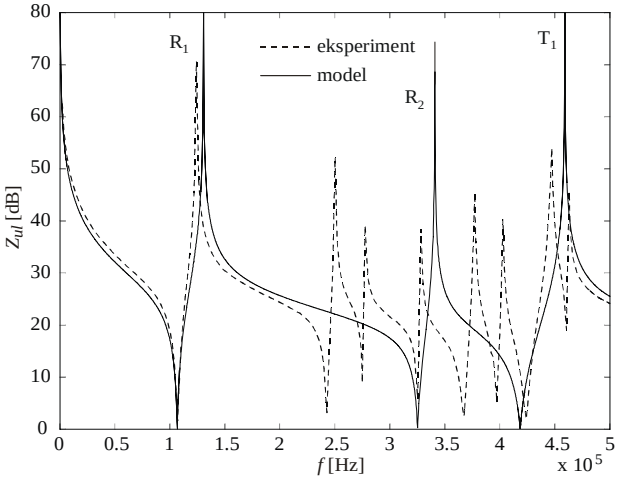

Figure 8.299. - *Electric impedance* $Z_{ul} = Z_{ul}(f)$

On Figure 8.300. is presented *characteristic of modulus of input electric impedance, simulated numerically on computer* in function of frequency, for PZT4 *piezoceramic circular plate* with dimensions $2a_2 = 38\,[mm]$, and $2h = 6{,}35\,[mm]$. It is assumed that oscillation is performed in air without additional external loading. On Figure 8.301. is presented comparison of numerically simulated on computer and measured experimental dependence of modulus of input electric impedance.

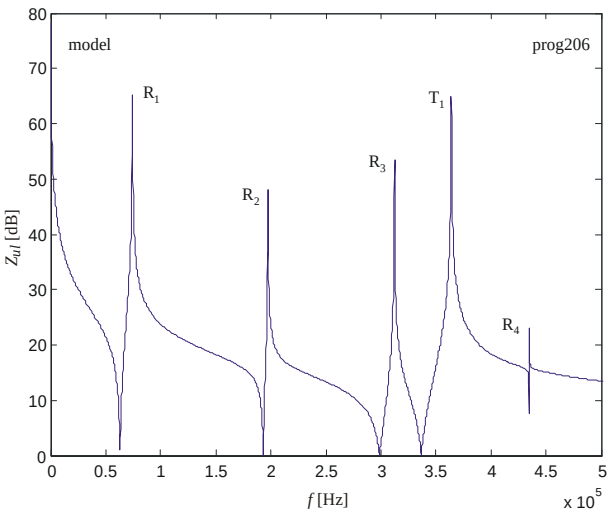

Figure 8.300. - *Electric impedance* $Z_{ul} = Z_{ul}(f)$

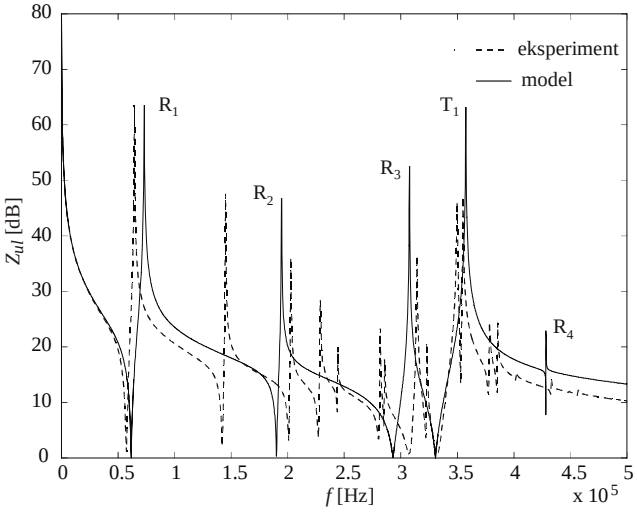

Figure 8.301. - *Electric impedance* $Z_{ul} = Z_{ul}(f)$

In case of piezoceramic circular plates, experimentally measured and numerically modelled dependences of electric impedance of frequency, in range of the first transversal mode T_1, even better coincide regarding the cases of circular-ring specimens, and satisfying results are also achieved in range of the first radial mode R_1. It is noticed that, considering *higher radial resonant modes* of oscillation R_2, R_3, R_4, R_5, …, *modelled resonant frequencies* of radial modes are mostly greater than measured ones, and rarely smaller than measured resonant frequencies (this conclusion stands for circular-ring plates and circular piezoceramic plates). One of possible causes for arising of this phenomenon is real presence of other types of oscillatory resonant modes, which are not encompassed by proposed and adopted model (for example: *edge mode of oscillation* and *flexion mode of oscillation – thickness-shear*), and which occur in region between the first radial R_1 and first transversal T_1 resonant mode of oscillation. Presence of other types of oscillatory modes is especially characteristic at piezoceramic specimens in shape of circular plates. This observation is best seen on Figure 8.299, where some resonant modes on experimental characteristic, in the vicinity of the modelled radial mode R_2, do not represent radial resonant

modes. Because the adopted model did not encompass these types of oscillation, *numerically modelled dependence of impedance* was mostly above experimentally measured characteristic, and it did not descend even at higher frequencies. Exception is the case of piezoceramic circular plate from Figure 8.297., where missing and not encompassed by model modes are poorly coupled with oscillatory modes present in model, so they have not great influence on electric impedance characteristic. Second possible cause of arising of the mentioned phenomenon is that model does not consider local mechanical and dielectric losses, occurrence of heating, and electrostriction of the piezoceramic element. Minimum and maximum values of electric impedance at resonant frequencies of radial and transversal oscillation are more distinct at calculated numerically modelled characteristic, regarding the experimentally obtained characteristic measured on automatic network analyzer HP4194A, at all analyzed cases of piezoceramic circular-ring plates and circular plates. Nevertheless all cited in the analysis, one can make a positive conclusion that, by proposed *and adopted* 3D *model*, generally in advance, even at design stage, one may predict the state of electric impedance with precise determination of frequencies of dominant, mutually coupled, resonant oscillatory modes. This conclusion is very important, as for theory and theory of experiment, as well as for the manufacturing technology, because one may predict behaviour of piezoceramic elements before their immediate workmanship, even at stage of calculation and design process.